

An Electrochemical Measurement for Evaluating the Cathodic Disbondment of Buried Pipeline Coatings under Cathodic Protection

Akvan, Farzaneh

Young Researchers and Elites Club, North Tehran Branch, Islamic Azad University, Tehran, IRAN

Neshati, Jaber^{*+}

*Industrial Protection Division, Research Institute of Petroleum Industry (RIPI),
P.O. Box 1485733111 Tehran, IRAN*

Mofidi, Jamshid

Chemistry Department, North Tehran Branch, Islamic Azad University, Tehran, IRAN

ABSTRACT: *Steel pipelines are susceptible to corrosion by the action of corrosive substance in the environment and one of the most common failure modes in buried pipeline coating is cathodic disbondment. Consequently, Electrochemical Impedance Spectroscopy (EIS) was used to assess the effect of three important parameters, the thickness of coating, the artificial defect and electrolyte type, on cathodic disbondment, according to ASTM G8. Experiments were done in 3.5 % wt NaCl, KCl and CaCl₂ solutions at room temperature with different coating thicknesses (354, 483 and 1014 μm) and several artificial defects diameters (3, 6 and 9 mm). Immersion time was 28 days and during this period, a -1.5 V cathodic potential (vs. SCE) was applied. Further, the EIS measurements were done in Open Circuit Potential (OCP). Investigations showed that a thick polyurethane coating was highly resistant to cathodic disbondment in intact areas and that coating thickness increases caused decreases in the rate of cathodic disbondment in areas with defects. On the other hand, the evaluation on artificial defects showed disputable results, though with no logical correlations between artificial defects' diameters and any disbonded area individually. In addition, assessment on electrolyte type showed the rate of cathodic disbonding might be classified after two parameters: solubility and mobility of ions. So, the disbonded area was dependent on the cation type in the electrolyte, and the anion diffusion had less effect in the cathodic disbondment process. Furthermore, the comparison between the cations and the anions in solution showed that the most important coating disbondments occurred when cations / anions are in a 1:1 ratio.*

KEY WORDS: *Cathodic disbondment; Corrosion; EIS; Pipeline; Cathodic Protection.*

* To whom correspondence should be addressed.

+ E-mail: neshatij@ripi.ir

1021-9986/15/2/83

7/\$/2.70

INTRODUCTION

Steel pipelines are susceptible to corrosion by the action of corrosive substance in the environment [1]. To reduce access of substances to the steel surface, organic coatings have been considered; a well selected coating can reduce the rate of corrosion to a negligible level, corrosion damage being thus prevented. A wide variety of organic coatings belonging to different functional groups have been used as external coatings for on-ground surface or buried pipelines. Polyurethane groups are one of the applicable products: they dry and cure rapidly, and come with good adhesion and endurance characteristics. After ASTM D16, they are a two-component product. However, 100% solid rigid aromatic polyurethanes are cheaper and often used for interior lining or buried applications [2].

Cathodic Disbondment (CD) is one of the most common failure modes in buried pipeline coating. While the coating membrane is still highly resistant [3,4], the disbondment, a loss of adhesion between an organic coating and its metal substrate, is due to the products of cathodic reduction reactions that take place in the interface of the coating [5]. Cathodic flow produces alkalinity at the interfaces, which causes discontinuities, either inherent or induced by the electrolyte in coating [6].

Cathodic Protection (CP) systems are installed to prevent corrosion of metal. Disbondment of coating occurs when coatings in a cathodic protection system interact either chemically or physically, ultimately causing corrosion beneath the layer [7]. Therefore, it is very important to perform CD tests when selecting coatings [8]. CD tests were developed in the 1960s and led to the publication of the ASTM G8-1969 standard, which defined which artificial defects to introduce in order to simulate the damaged area of a coating [9-11]. Many studies have been dedicated to this subject regarding the mechanisms of CD of organic coatings on steel [12-17].

Pipeline corrosion and Stress Corrosion Cracking (SCC) occur in electrolytes developed under disbonded coatings [18-23]. Corrosion of steel under disbonded coatings has been assessed using various electrochemical measurement techniques. Computational simulation [24-28] and EIS technique have been extensively used to study the coating performance and determine the corrosion of steel under the coating [29-33].

EXPERIMENTAL SECTION

Specimen preparation

Carbon steel panels (SAE 1020) were utilized as a substrate. The steel panels (100×150×2mm) were prepared in accordance with ISO 8501-1, grade Sa 2.5(SIS 055900-67) to give a medium profile in accordance with EN ISO 8503-2 innuendo profile of 75μm, then, degreased with toluene before being painted with thick 100% solid rigid aromatic polyurethane (ASTM D16, D1186, D4366, D4541), our polyurethane was supplied by Madison Company, which is a commercial brand, and coating applied by brushing, the coating system does not use any solvent to dissolve it, carry or reduce any of the coating resins. Furthermore, the resins normally still in liquid state will convert, 100%, to a solid film after application.

Then, a hole was drilled through the center of each specimen through the coating to the substrate. The depth of the hole was adjusted to ensure that no coating was visible within the area of the defect, and excessive penetration into the steel substrate was avoided.

Designing the electrochemical cells

Electrochemical cells were designed to separate the measurements of the cathodic disbondment process from the influence of the impedance of an artificial defect. The reliability of the experimental setup (double cell) shows that the cell does not influence the disbondment process in a significant way. An outer electrolyte cell was made of a 62-mm diameter glass cylinder on the top of the coating and was glued with silicone rubber. A smaller, 30-mm diameter glass cylinder was also glued around the artificial defect to form an inner electrolyte. The exposed surface area between the inner and outer cylinders (intact area) was 23 cm², and the inner cell area, including the artificial defect, was 7 cm². The cell was filled with electrolytes. The level of the electrolytes was kept unchanged with distilled water during the immersion time.

A three-electrode system was used for the measurements of electrochemical impedance spectroscopy. The specimen of coated steel was used as the working electrode, a platinum net as a counter electrode (50×10mm); a Saturated Calomel Electrode (SCE) was used as a reference electrode. The reference electrode was constructed from glass with a porous plug,

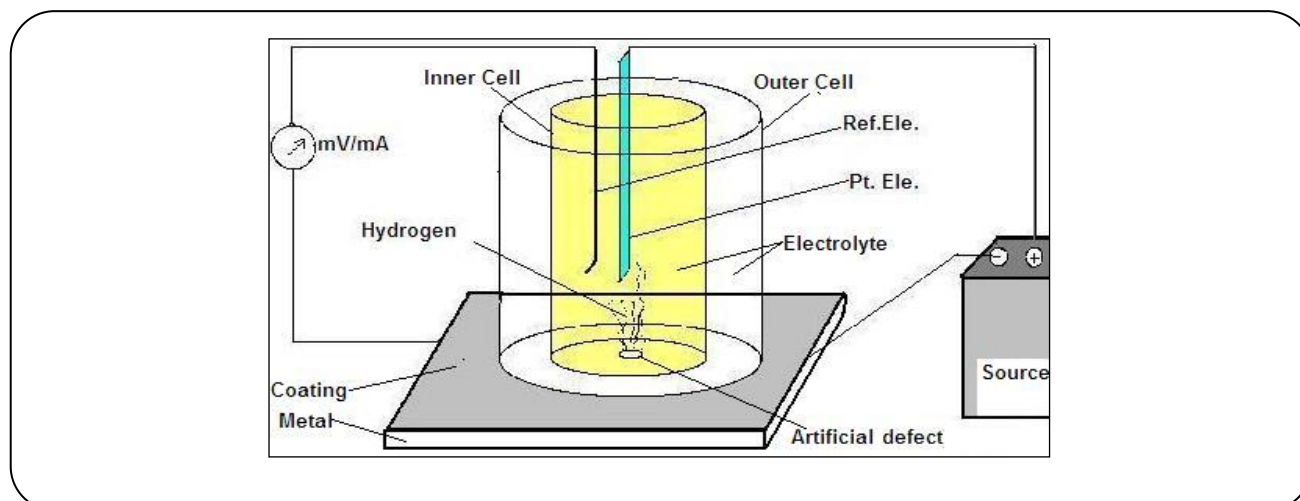


Fig.1: Schematics of the electrochemical cell.

and the diameter of the plug was less than 10 mm. It was located within 20 mm from the anode; the anode was fixed perpendicularly, at 10 mm above the defect. During the test without AC impedance measurement, a -1.5 V cathodic potential versus SCE was applied on both the inner and outer cells.

Testing method

Experiments were performed in 3.5 % wt NaCl, KCl and CaCl₂ solutions at room temperature with different thicknesses of coating (354, 483 and 1014 μm) and different diameters of artificial defect (3, 6 and 9 mm). Fig.1 displays schematics of the electrochemical cell.

Electrochemical and visual measurement

The EIS measurements were performed by the Potentiostat / Galvanostat Model 273A and SI 1255 (high frequency response analyzer). Further, the EIS measurements were carried out at the Open Circuit Potential (OCP), with a 5mV AC amplitude potential, in the 10 kHz - 5mHz range. The analysis of impedance data was performed using the well-known Z-view computer analysis program.

After a 28-day immersion, the cylinders were removed, and the specimen was washed with water and dried, then, examined as follows: six radial incisions were made through the coating to the substrate, which extended outwards from the defect for at least 30 mm and at an angle of approximately 60° from each other. The knife point was inserted under the sections; a gentle

levering action was used to slowly pull each section away until a firm adhesion was reached. Finally, disbonded areas were evaluated via paper.

RESULTS AND DISCUSSION

Electrochemical impedance measurement

Impedance diagrams were measured for the coating system at various intervals over the 28-day immersion period.

Research findings have shown that more corrosion resistance coatings have resistance values of the order of 10⁸-10¹⁰ Ω.cm² and capacitance values of the order of 10⁻¹⁰ F/cm². Relatively poor corrosion protection occurred when impedance decreased below 10⁵ Ω.cm² and the capacitance values settled in the upper microfarads per square centimeter range [34]. The impedance diagram obtained for coating system of outer cell (intact area) and inner cell (disbonded area) to the frequency of 10 kHz-5mHz is shown in Fig.2. Accordingly, coating system had good corrosion resistance in intact areas. R_f represents the sum of coating resistance, the charge transfer resistance and the solution resistance: this is called "pore resistance" as referred to in Mansfeld & Kending [35].

In Fig.3, three specimens were selected (specimen B: 354 μm in NaCl, specimen E: 1.18 μm in NaCl, specimen G: 363 μm in KCl), changes of R_f are shown for coating during the immersion time. All of the outer cells are indicated as "high resistance", thanks to the good adhesion. Obtained curve shows that the coating system is highly resistant to corrosion. Usually, R_f decreases

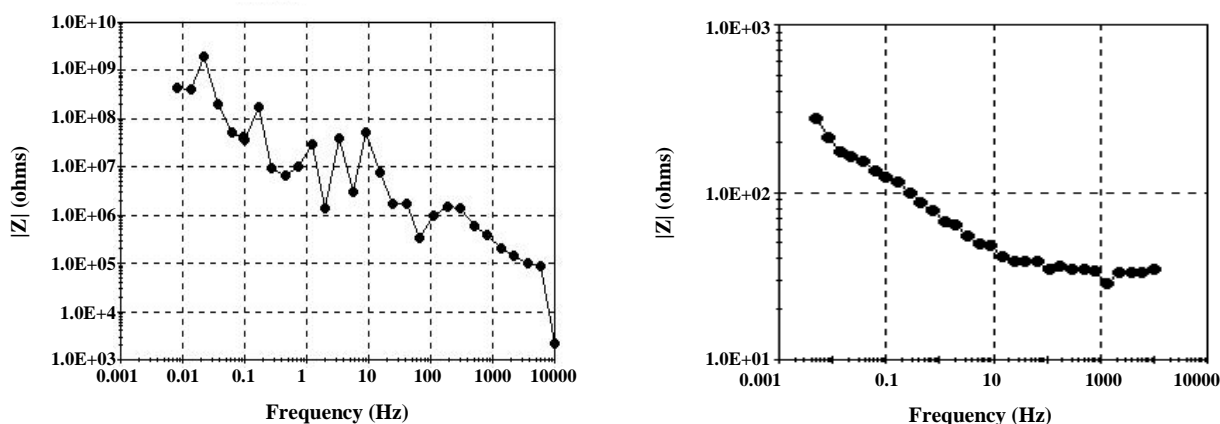


Fig. 2: Bode $|Z|$ diagram, a. Outer cell (Intact area), b. Inner cell (Disbonded area) after a 28 day immersion.

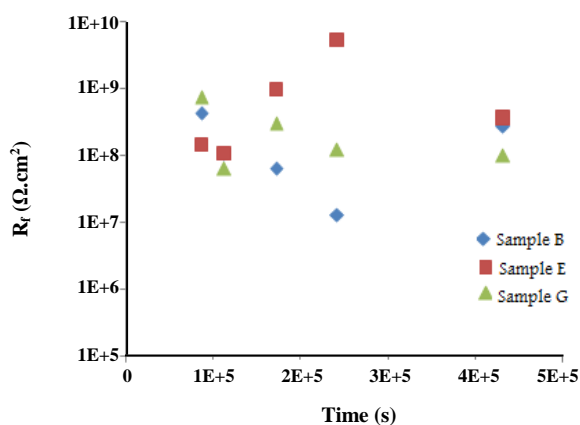


Fig. 3: Fluctuations of R_f during time (Coating thickness, artificial defects diameter, electrolyte consecutively in: specimen B: 345 μm , 6mm, NaCl; specimen E: ~1015 μm , 9mm, NaCl; specimen G: 363 μm , 6mm, KCl)

during the degradation of the coating and, therefore, would cause a gradual increase in the corrosion rate of the substrate. However, sometimes, when the R_f parameter increases with time, it means that the rate of corrosion on the substrate decreases. This problem goes back to the mechanism of corrosion and the formation of corrosion products during the damage process [36-37].

Effect of coating thickness

In the evaluation of the coating thickness, based on Table 1, it is shown that disbonded area decreases when coating thickness increases in areas with defect.

In addition, the analysis of EIS curves in break point frequency ($\theta = -45$) shows that the thickness of coating is an efficient factor of the cathodic disbondment, Fig 4, Table 1.

Impedance plots showed scattered results at the beginning of the experiments, but the system reached a steady state after a 24-hour immersion. There was no visible degradation or disbondment at this stage. However, the AC impedance dropped dramatically; water accumulated enough at the coating–steel interface to maintain the cathodic reaction: this is an essential reaction for cathodic disbondment [38-45].

The fluctuations of the open circuit potential (E_{ocp}) over time indicated the negative trend. It seemed that the diffusion of corrosive ions and water absorption under the well adhered area were increasing. Thus, the steel corrosion reactions sped up. It could be the result of electrolyte penetration in the coating and degradation of coating, or of the degradation of the double-layer capacitance. Very noisy AC impedance was observed, due to the diffusion of electrolytes into the coating. The biggest influence was observed between the fifth and thirteenth days based on EIS plots. It is obvious that the diffusion of electrolytes is dependent on the coatings thickness and on environmental factors.

pH value increases due to the entrance of OH^- ions into the solution and the alkalinity also increases (Fig.5, Table 1). Alkalinity reduces water activity, and an osmotic pressure gradient on the coating-metal is formed, which causes blisters and cathodic disbondment of coating.

According to the EN 10290 and JFE [46-48] standards, it is mentioned the separation rate was equal to or less than a 10- to 15-mm radius. Thus, the separation rate for the coating was acceptable.

Table 1: Evaluation of coating thickness after a 28 day immersion (In NaCl solution and 6mm diameter of defect).

Specimen	Coating Thickness (μm)	Equivalent circuit diameter (mm)	Disbonded area (mm^2)	Frequency in $\theta = -45$ High frequency (Hz)	Frequency in $\theta = -45$ Low frequency (Hz)
B	354	22.94	413.50	3.34	0.034
A	483	19.02	284.07	0.01	0.01
D	1014	10.91	93.49	0.005	0.005

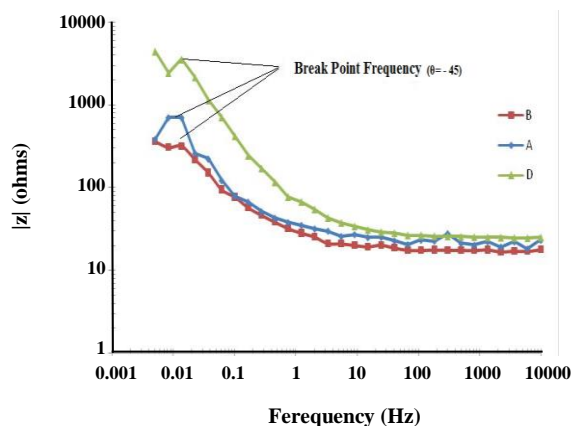


Fig.4: $|Z|$ versus frequency to show break point frequency in three different thickness of coating (specimen B: $345\mu\text{m}$, specimen A: $483\mu\text{m}$, specimen D: $1014\mu\text{m}$, In NaCl solution and 6mm diameter of defect).

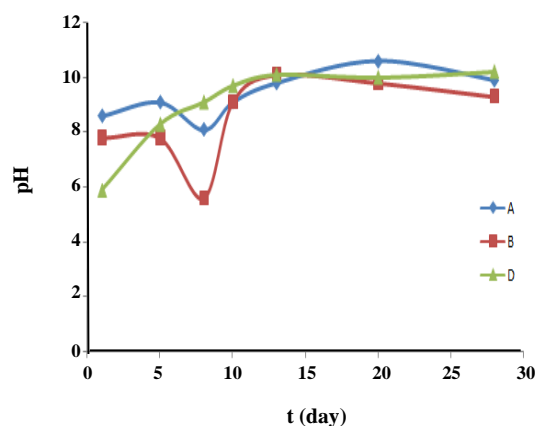


Fig. 5: pH measurements during the time

Effect of the artificial defect

The artificial defect was investigated with three diameters according to Table 2. In the same condition such as NaCl solution and coating thickness $\sim 1015\mu\text{m}$, specimen D with 6mm artificial defect has shown the highest disbondment. However, systematically, specimens F and E with 3 and 9mm artificial defects showed the lowest disbondment. This means the artificial defect is a major factor of the cathodic disbondment coating process, but with no logical correlations between artificial defects' diameters and any disbonded area individually.

Effect of electrolyte type

In order to evaluate the electrolyte type, 3.5 %wt NaCl, KCl and CaCl_2 solutions were used (Table 3). All tests have been performed in accelerated corrosion condition in laboratory; the level of concentration of chlorides were often selected to simulate chloride concentration of seawater which has a salt concentration is about 3.5% wt and regarding accelerated corrosion tests there is no mention about capacity of ions.

Accordingly, it has been shown that the current passing through the metal can free hydrogen atoms and cause coating disbondment. It seems that the type of electrolyte is one of the other efficient parameters in disbondment. In electrolyte evaluation, the rate of cathodic disbonding may be classified after two parameters: solubility and mobility of ions. The disbonded area was the smallest in a specimen with CaCl_2 electrolyte. It seems the electrolyte structure, its white sediments and corrosion products avoid the penetration of Ca^{+2} and Cl^- ions in the coating. This is likely due to the low solubility of hydroxides of divalent cations, here, Ca^{+2} . Further, in this specimen, the outing of OH^- ions from cathodic reactions is very slow. Therefore, when compared with other electrolyte types through visual inspections, it shows that the exit of OH^- ions from the cathode reactions is very slow. The specimens with KCl electrolyte have a higher disbondment rate than in NaCl solutions; therefore, disbonded areas depend on the cation type in the electrolyte. The anion diffusion has less effect in the cathodic disbondment process, as negative OH^-

Table 2: Evaluation of artificial defect after a 28 day immersion (In NaCl solution and coating thickness ~1015 μm).

Specimen	Diameter of defect (mm)	Equivalent circuit diameter (mm)	Disbonded area (mm^2)
E	9	10.26	82.70
D	6	10.91	93.49
F	3	10.15	80.90

Table 3: Evaluation of electrolyte type effect (Coating thickness ~ 370 μm and 6mm diameter of defect).

Specimen	Electrolyte	Equivalent circuit diameter (mm)	Disbonded area (mm^2)
G	KCl	27.84	608.59
B	NaCl	22.94	413.52
H	CaCl_2	4.78	17.97

ions are already present on the metal surface, due to the cathodic electrochemical reaction. Therefore, only the positive ions should diffuse through the coating or through the defect in order to balance the charge.

Mobility of the cations is different. Therefore, this leads to different hydrated cations dimensions. Actually, although the atomic number of K is higher than the atomic number of Na, it occurs that the hydrated Na^+ ion is larger than the K^+ ion (Na^+ ion radius is 0.102 nm and K^+ is 0.138 nm, when the Na^+ hydrated ion radius is 0.79 nm and K^+ is 0.53 nm) [49]. In many studies, the mobility of the cation follows a linear relationship with the rate of cathodic disbanding [50]. Na^+ may diffuse through the defect area only, when K^+ can diffuse through the defect area and the coating. This can cause an increase in the cathodic disbondment. Considering the cations migrating towards the cathodically protected substrate, approximately 1/3 of these cations diffused through the intact coating while 2/3 migrated in and through the defect area [51]. Thus, the results revealed the most coating disbondments occurred when cations / anions are in a 1:1 ratio.

Fluctuations of the open circuit potential (E_{ocp}) over time indicated a negative trend, which showed that water absorption under the intact area was increasing. Hence, the reactions of carbon steel corrosion were also increased: this could be the result of electrolyte penetration in the coating and of its subsequent degradation, or of the degradation of the double-layer capacitance. In the specimen with CaCl_2 electrolyte, E_{ocp} is almost constant over time. Thus, the separation rate of the coating is almost constant (Fig.6, Table.3).

CONCLUSIONS

Regarding accelerated procedures to assess coating delamination resistance for protecting pipeline coatings, ASTM G 8 remains a good candidate for simultaneously determining comparative characteristics, thanks to the useful data it provides. In this research, three parameters, the coating thickness, the artificial defect and the electrolyte type were investigated according to the ASTM G8 standard using Electrochemical Impedance Spectroscopy (EIS). The investigations showed the thick polyurethane coating can be highly resistant to cathodic disbondment in intact areas. If there was no coating defect (intact area), cathodic disbondment did not occur in a short time. It means more corrosion resistance coatings have resistance values of the order of 10^8 – 10^{10} $\Omega\cdot\text{cm}^2$ and capacitance values of the order of 10^{-10} F/cm^2 . Further, evaluation on coating thickness showed that disbonded area decreases along with a coating thickness increase in areas with defect. On the other hand, the evaluation on artificial defects showed disputable results, though with no logical correlations between artificial defects' diameters and any disbonded area individually. In addition, assessment on electrolyte type showed the rate of cathodic disbonding might be classified after two parameters: solubility and mobility of ions. So, the disbonded area was dependent on the cation type in the electrolyte, and the anion diffusion had less effect in the cathodic disbondment process. Furthermore, the comparison between the cations and the anions in solution showed that the most important coating disbondments occurred when cations / anions are in a 1:1 ratio.

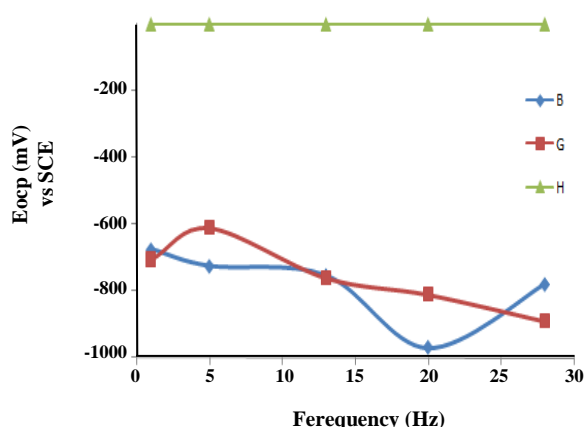


Fig. 6: Fluctuations of measured potential during time (Coating thickness $\sim 370 \mu\text{m}$ and 6mm diameter of defect, electrolyte in specimen B: NaCl, specimen G: KCl, specimen H: CaCl₂).

Acknowledgements

The authors gratefully acknowledge the cooperation provided by Mr. Patrick Dubosc and the support by the Research Institute of Petroleum Industry (RIPI).

Received : Oct. 19, 2014 ; Accepted : Mar. 2, 2015

REFERENCES

- [1] Norsworthy R, Understanding Corrosion in Underground Pipelines: Basic Principles, *Underground Pipeline Corrosion J.*, 3-34 (2014)
- [2] Guan S.W., %100 Solid Polyurethane and Polyurea coatings technology, *Coatings World*, 49-58 (2003).
- [3] Yan M., Wang J., Han E., ke W., Local Environment under Simulated Disbonded Coating on Steel Pipelines in Soil Solution, **50**: 1331-1339 (2008).
- [4] Chen X., Li. X.G., Du C.W., Cheng Y.F., [Effect of Cathodic Protection on Corrosion of Pipeline Steel under Disbonded Coating](#), *Corrosion Science*, **51**: 2242-2245 (2009).
- [5] Fu A.Q., Cheng Y.F., [Characterization of Corrosion of X65 Pipeline Steel under Disbonded Coating by Scanning Kelvin Probe](#), *Corrosion Science*, **51**: 914-920 (2009).
- [6] Luo J., Lin C., Yang Q., Guan S., [Cathodic Disbonding of a Thick Polyurethane Coating from Steel in Sodium Chloride Solution](#), *Progress in Organic Coatings*, **31**: 289-295 (1997).
- [7] Deflorian F., Rossi S., [An EIS Study of Ion Diffusion Through Organic Coatings](#), *Electrochimica Acta*, **51**: 1736-1744 (2006).
- [8] Changjun C., Qiao P., Study on Hydrogen Permeation Process, **209**: 1011-1015 (2003).
- [9] Zhang J., Hu J., Cao C., Studies of Impedance Models and Water Transport Behaviors of Polypropylene Coated Metals in NaCl Solution, *Progress in Organic Coatings*, **49**: 293-301 (2004).
- [10] Neshati J., Rezaei F., Akbarinezhad E., Evaluation of Protection Against Corrosion of Thick Polyurethane Coating by Electrochemical Impedance Spectroscopy, *Surface Engineering*, **24**: 470-474 (2008).
- [11] Luo J., Lin C., Yang Q., Guan S., [Cathodic Disbonding of a Thick Polyurethane Coating from Steel in Sodium Chloride Solution](#), *Progress in Organic Coatings*, **31**: 289-295 (1997).
- [12] Watts J., Mechanistic Aspects of the Cathodic Delamination of Organic Coatings, *The Journal of Adhesion*, **31**: 73-85 (1989).
- [13] Flavio D., Stefano R., [An EIS Study of Ion Diffusion Through Organic Coatings](#), *Electrochimica Acta*, **51**: 1736-1744 (2006).
- [14] Skar J., Steinsmo U., Cathodic Disbonding of Pain Films-Transport of Charge, *Corrosion Science*, **35**: 1385-1389 (1993).
- [15] Horner M., Boerio F., Cathodic Delamination of an Epoxy/Polyamide Coating from Steel, *The Journal of Adhesion*, **32**: 141-156 (1990).
- [16] Stratmann M., Leng A., Fürbeth W., Streckel H., Gehmecker H., [The Scanning Kelvin Probe; A New Technique for the in Situ Analysis of the Delamination of Organic Coatings](#), *Progress in Organic Coatings*, **27**: 261-267 (1996).
- [17] Rohwerder M., Hornung E., Stratmann M., Microscopic Aspects of Electrochemical Delamination: an SKPFM Study, *Electrochimica Acta*, **48**: 1235-1243 (2003).
- [18] Cheng Y.F., Niu L., [Mechanism for Hydrogen Evolution Reaction on Pipeline Steel in Near-Neutral pH Solution](#), *Electrochemistry Communications*, **9**: 558-562 (2007).
- [19] Parkins R.N., Uhlig's Corrosion Handbook, 2nd edition, Revie R.W. (Editor), Wiley, New York, 191-194 (2000)
- [20] Niu L., Cheng Y., Corrosion Behavior of X-70 Pipe Steel in Near-Neutral pH Solution, *Applied Surface Science*, **253**: 8626-8631 (2007).

- [21] Cheng Y., Thermodynamically Modeling the Interactions of Hydrogen, Stress and anodic Dissolution at Crack-Tip During Near-Neutral pH SCC in Pipelines, *Journal of Materials Science*, **42**: 2701-2705 (2007).
- [22] Dong C., Fu A., Li X., Cheng Y., [Localized EIS Characterization of Corrosion of Steel at Coating Defect under Cathodic Protection](#), *Electrochimica Acta*, **54**: 628-633 (2008).
- [23] Leidheiser H., The Mechanism for the Cathodic Delamination of Organic Coatings from a Metal Surface, *Progress in Organic Coatings*, **11**: 19-40 (1983).
- [24] Van Der Weijde D., Van Westing E., De Wit J., [Electrochemical Techniques for Delamination Studies](#), *Corrosion Science*, **36**: 643-652 (1994).
- [25] Perdomo J., Song I., Chemical and Electrochemical Conditions on Steel Under Disbonded Coatings: the Effect of Applied Potential, Solution Resistivity, Crevice Thickness and Holiday Size, *Corrosion Science*, **42**: 1389-1415 (2000).
- [26] Perdomo J., Chabica M., Song I., [Chemical and Electrochemical Conditions on Steel under Disbonded Coatings: the Effect of Applied Potential, Solution Resistivity, Crevice Thickness and Holiday Size](#), *Corrosion Science*, **43**: 515-532 (2001).
- [27] Fu A., Cheng Y., Characterization of Corrosion of X65 Pipeline Steel under Disbonded Coating by Scanning Kelvin Probe, *Corrosion Science*, **51**: 914-920 (2009).
- [28] Jorcin J., Aragon E., Merlatti C., Pébère N., [Delaminated Areas Beneath Organic Coating: A Local Electrochemical Impedance Approach](#), *Corrosion Science*, **48**: 1779-1790 (2006).
- [29] Mansfeld F., Use of Electrochemical Impedance Spectroscopy for the Study of Corrosion Protection by Polymer Coatings, *Journal of Applied Electrochemistry*, **25**: 187-202 (1995).
- [30] F. Mansfeld, Models for the Impedance Behavior of Protective Coatings and Cases of Localized Corrosion, *Electrochimica Acta*, **38**: 1891-1897 (1993).
- [31] Lee C., Mansfeld F., [Automatic Classification of Polymer Coating Quality using Artificial Neural Networks](#), *Corrosion Science*, **41**: 439-461 (1998).
- [32] Alavi S.M., Mirmomen M., Experimental Study of Coating in a Bottom Sprayed Fluidized Bed, *Iran. J. Chem. Chem. Eng. (IJCCE)*, **26**: 37-44 (2007)
- [33] Deflorian F., Rossi S., The Role of Ions Diffusion in the Cathodic Delamination Rate of Polyester Coated Phosphatized Steel, *Journal of Adhesion Science and Technology*, **17**: 291-306 (2003).
- [34] Mahjani M., Neshati J., Masiha H., Ghanbarzadeh A., Jafarian M., Evaluation of Corrosion Behaviour of Organic Coatings with Electrochemical Noise and Electrochemical Impedance Spectroscopy, *Surface Engineering*, **22**: 229-234 (2006).
- [35] Neshati J., Fardi M., Evaluation and Investigation of Surface Treatment of Industrial Coatings by Impedance Spectroscopy, *Surface Engineering*, **20**: 299-303 (2004).
- [36] Nguyen T., Martin J., Modes and Mechanisms for the Degradation of Fusion-Bonded Epoxy-Coated Steel in a Marine Concrete Environment, *Journal of Coatings Technology and Research*, **1**: 81-92 (2004).
- [37] Eng A., Pilgrim F., Patel M., "Mechanisms of Military Coatings Degradation", End of Fiscal Year Report (2000).
- [38] Lee S.H., Oh W.K., Kim J.G., Acceleration and Quantitative Evaluation of Degradation for Corrosion Protective Coatings on Buried Pipeline: Part I. Development of Electrochemical Test Methods, *Progress in Organic Coating*, **76**(4): 778-783 (2013).
- [39] Afshari V., Dehghanian C., [Electrochemical Polarization and Passivation of Nanostructured Iron in Acid Solution](#), *Anti-Corrosion Methods and Materials*, **57**: 142-147 (2010).
- [40] Pistorius P., Burstein G., [Aspects of the Effects of Electrolyte Composition on the Occurrence of Metastable Pitting on Stainless Steel](#), *Corrosion Science*, **36**: 525-538 (1994).
- [41] Ritter J., Rodriguez M., An Electrochemical and Sers Study, *Corrosion Science*, **38**: 223-226 (1982).
- [42] Atkinson J., Granata R., Leidheiser Jr H., McBride D., Cathodic Delamination Of Methyl Methacrylate-Based Dry Film Polymers On Copper, *IBM Journal of Research and Development*, **29**: 27-36 (1985).
- [43] McCafferty E., Hubler G., Natishan P., Moore P., Kant R., Sartwell B., *Materials Science and Engineering*, **86**: 1-17 (1987).

- [44] McCafferty E., [Thermodynamic Aspects of the Crevice Corrosion of Iron in Chromate/Chloride Solutions](#), *Corrosion Science*, **29**: 391-401 (1989).
- [45] Chuang T., Nguyen T., Lee S., Micro-Mechanic Model for Cathodic Blister Growth in Painted Steel, *Journal of Coatings Technology*, **71**: 75-85 (1999).
- [46] "Steel Tubes and Fitting for Onshore and Offshore Pipelines-External Applied Liquid Polyurethane and Polyurethane Modified Coatings", BS EN 10290, London, UK (2002).
- [47] "Recent Corrosion Protective Steel Pipes", JFE Technical Report No.7, Available at <http://www.jfesteel.co.jp/en/research/report/007/pdf/007-15.pdf> (2006).
- [48] Berry R.S., Rice S.A., Ross J., "Physical Chemistry", J. Wiley & Sons, New York (1980).
- [49] "Physical Chemistry", Oxford University Press, Oxford (1987).
- [50] O. Ø. Knudsen, J. I. Skar, "Cathodic Disbonding og Epoxy Coatings - Effects of Test Parameters", Corrosion 2008, Paper 08005 (Houston, TX: NACE (2008).
- [51] Deflorian F., Rossi S., The role of Ions Diffusion in the Cathodic Delamination Rate of Organic Coated Steel, *Journal of Adhesion Science and Technology*, **17**: 291-306 (2003).